A Sensorless Control of Four Switch BLDC Motor Drive

Geethu James
M.Tech Student,
Department of Electrical and Electronics Engineering,
Mar Athanasius College of Engineering, Kothamangalam,686666(Kerala), India.

Prof. K Radhakrishnan
Head of the Department,
Department of Electrical and Electronics Engineering,
Mar Athanasius College of Engineering, Kothamangalam,686666(Kerala), India.

Mrs.Jaya B
Scientist
CECG
VSSC
Trivandrum, 695022(Kerala), India.

Abstract

This paper describes the analysis and design of a low cost three phase inverter brushless dc motor (BLDC) drive. The proposed method is a cost effective sensorless method employed for four switch BLDC motor. The absence of hall sensors give rise to a sensorless control in which the commutation instants are obtained from the zero crossing points (ZCP) of three voltage functions that are derived from the filtered stator terminal voltages V_{ao} and V_{bo}. Hence phase shifters are not required that are common in conventional sensorless methods. The average terminal voltages are calculated using two low pass Butterworth filters. The phase currents are controlled using direct phase current (DPC) control scheme. The simulation results give the performance of developed sensorless technique.

Index Terms—Brushless DC(BLDC) motor drive, four-switch inverter,Sensorless control, phase shift.

I. Introduction.

Permanent-magnet Brushless DC(PMBLDC) motors with trapezoidal back emf finds a variety of applications in aerospace, automotives, industries, military, computers, household products etc. due to higher efficiency, higher torque, higher power factor, increased power density, ease of construction ,ease of control and ease of maintenance. The torque developed by a BLDC motor is constant as they are generated from trapezoidal back EMF and quasi square-wave currents. A conventional Brushless DC motor is excited by a six switch three phase inverter (SSTPI) where commutation is achieved through an inverter and a position sensor. So for each electrical cycle, three Hall-effect position sensors placed 120° apart on the stator provides the six commutation instants. Researchers are always conscious about their cost and are always exploring methods to bring in cost minimization. Cost effectiveness can be achieved either by reducing the number of power switches used in the inverter circuit, called topological approach or by proper designing of algorithms and their implementation in conjunction with a reduced component converter, called the control approach.

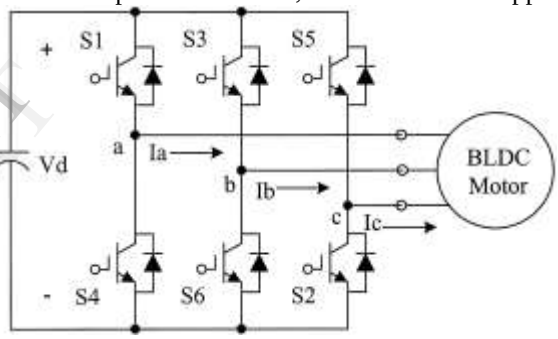

Fig.1 Conventional six-switch three phase BLDC motor drive.

In this paper cost effectiveness is achieved by reducing the number of power switches, switching driver circuits, dc power supplies, total price and losses. A BLDC motor can be controlled by sensored control or sensorless control method. But for reducing the manufacturing cost a feasible sensorless method is developed by eliminating the position sensors. Also in harsh environments where these sensors cannot function reliably sensorless control is the only choice. In conventional six switch inverter topology a 30° phase delay is to be carried out between the zero crossing point of back emf and the commutation instant. In this aspect too four switch topology minimizes the cost by using the ZCP of three voltage functions, that coincide to six commutation instants rather than using complicated hardware's to carry out phase shift. Theoretical analysis and simulations on MATLAB/SIMULINK

were conducted to demonstrate the feasibility of the proposed sensorless method.

II. Analysis of a FSTPI-BLDC motor drive.

The configuration of a four-switch three phase inverter (FSTPI) BLDC motor is shown in fig 2. The equivalent circuit of the four switch inverter Brushless DC motor drive is shown in figure 3.

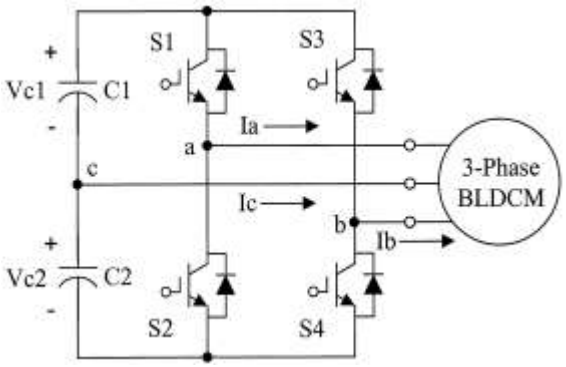

Fig.2.Proposed four switch three phase BLDC motor drive.

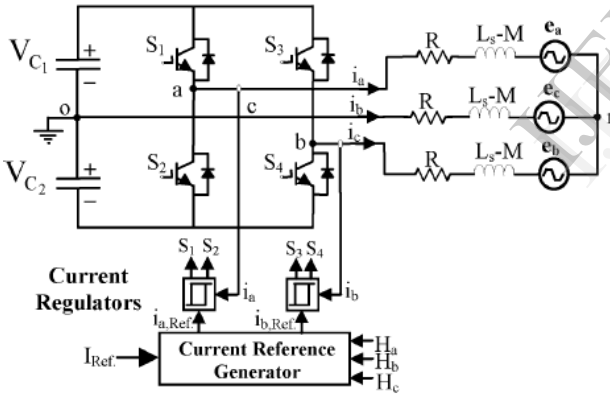

Fig.3.Equivalent circuit of FSTPI BLDC motor drive.

The equation of a typical BLDC motor is represented as follows:

$V_{an}=R*i_a + (L_s-M)\, d/dt\, (i_a) + e_a$

$V_{bn}=R*i_b + (L_s-M)\, d/dt\, (i_b) + e_b \quad (1)$

$V_{cn}=R*i_c + (L_s-M)\, d/dt\, (i_c) + e_c$

Where V_{xn}, R, i_a, e_a, L_s and M represents the phase voltages, resistances, phase currents,self inductances and mutual inductances of phase x,respectively(x=a, b, c).The six operating modes for FSTPI BLDC motor drive are shown in fig.4.

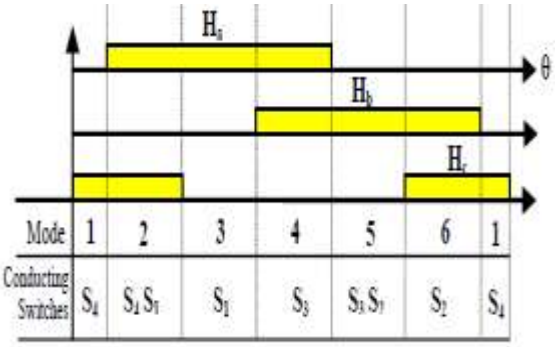

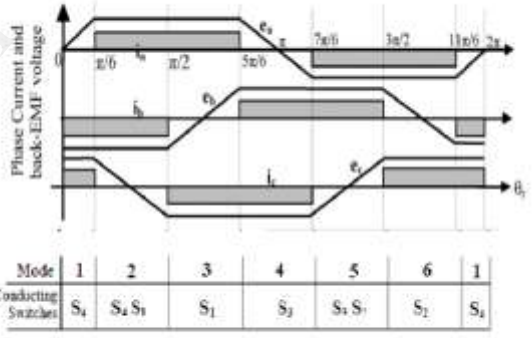

Fig 4.Phase current and trapezoidal back emf of BLDC motor with hall sensor signals.

A. Four-switch converter for BLDC motor drives.

In the four-switch configuration, the four switching status as shown in figure 5 are (0, 0), (0, 1), (1, 0), and (1, 1) where "0" means the lower switch is turned on and "1" means the upper switch is turned on.In the case of six-switch converter,the switching status (0,0) and (1,1) cannot supply the DC –link voltage to the load.So the current cannot flow through the load at these instants and hence they are regarded as zero vectors.

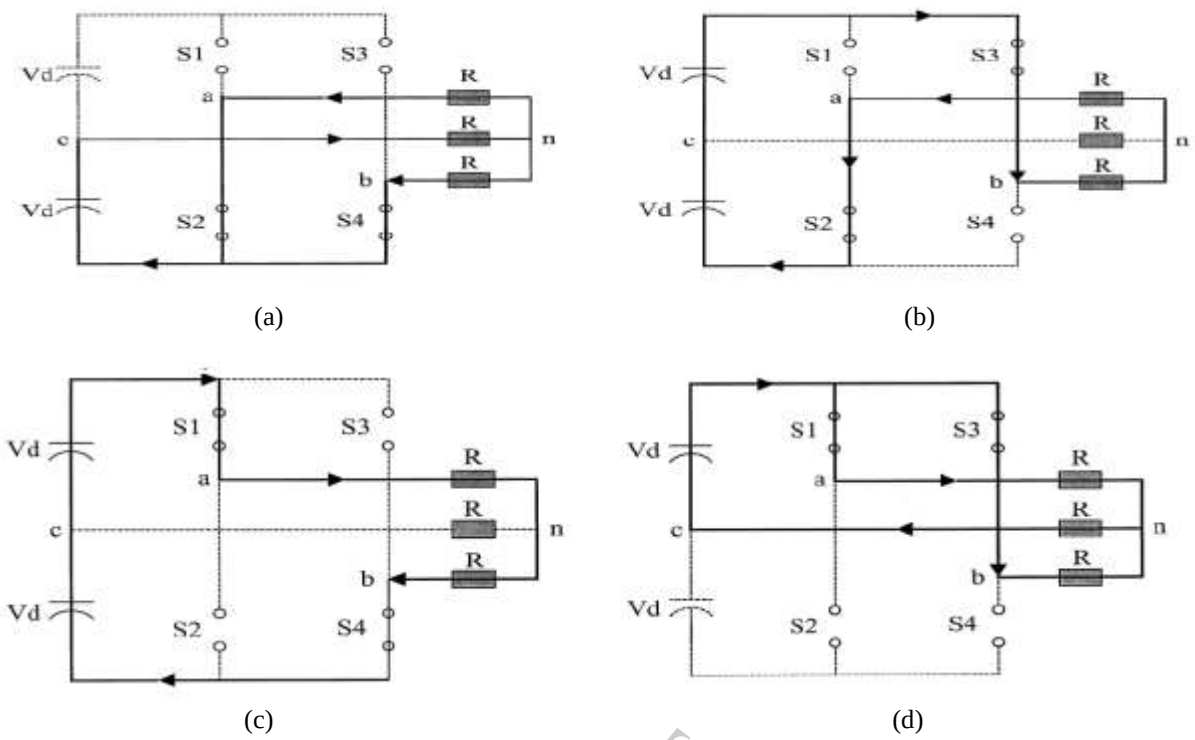

Fig 5.Voltage vectors of four switch converter with resistive load: (a)(0,0) vector, (b)(0,1) vector, (c)(1,0) vector, (d)(1,1) vector.

However, in the four-switch converter, current is flowing even at the zero-vectors as one phase of the motor is always connected to the midpoint of the dc-link capacitors. Moreover, the phase which is connected to the midpoint of dc-link capacitors is uncontrolled and only the resultant current of the other two phases flow through this phase during the switching status (0, 1) and (1, 0).This current is treated as zero if load is considered to be ideally symmetrical.

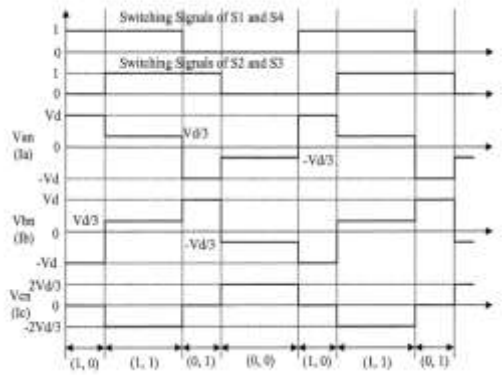

Fig 6.Voltage and current waveforms based on four switching vectors for four switch converter.

For a BLDC motor to generate maximum and constant output torque, their phase currents should be rectangular with 120° conducting and 60° non-conducting intervals. Also at each operating mode, only two phases are conducting and the other phase remains silent or inactive. However, in the four-switch converter based on the four switching vectors as shown in figure 6,the generation of 120° conducting and a 60° non-conducting current profiles is inherently difficult. That means the conventional PWM schemes employed for four switch induction motor drives cannot be directly applied to BLDC motor drives. This led to the development of a new control scheme called Direct Current Controlled PWM scheme.

B. Direct current controlled PWM scheme.

Under a balanced condition, the three-phase currents will satisfy the following condition:

$I_a + I_b + I_c = 0$ (2)

This can also be written as

$I_c = -(I_a + I_b)$ (3)

In an ac induction motor drive, at any instant there are always three phase currents flowing as:

$I_a \neq 0; I_b \neq 0; I_c \neq 0$ (4)

But from Fig.4, for a BLDC motor (4) is not valid anymore. Table I indicate the detailed current equations from their corresponding operating modes. Due to the characteristics of BLDC motor, only two phases need to be controlled by the four switches using the hysteresis current control method during

Table I
Detailed current equations from the operating modes of BLDC motor.

Mode I (0°<θ<30°)	$I_b + I_c = 0$ and $I_a = 0$
Mode II (30°<θ<90°)	$I_a + I_b = 0$ and $I_c = 0$
Mode III (90°<θ<150°)	$I_a + I_c = 0$ and $I_b = 0$
Mode IV (150°<θ<210°)	$I_b + I_c = 0$ and $I_a = 0$
Mode V (210°<θ<270°)	$I_a + I_b = 0$ and $I_c = 0$
Mode VI (270°<θ<330°)	$I_a + I_c = 0$ and $I_b = 0$

each operating mode. Hence this scheme is called the Direct Current Controlled PWM scheme.This is shown in table I.

Table II
Switching sequences of four switch converter

Modes	Active Phases	Silent Phases	Switching Devic
Mode I	Phase B and C	Phase A	S4
Mode II	Phase A and B	Phase C	S1 and S4
Mode III	Phase A and C	Phase B	S1
Mode IV	Phase B and C	Phase A	S3
Mode V	Phase A and B	Phase C	S2 and S3
Mode VI	Phase A and C	Phase B	S2

C. Current regulation.

Current is regulated to obtain the required quasi-square waveform. Based on the switching sequences shown in table II, the current regulation is brought out by hysteresis current control scheme. The switching sequence and corresponding current flow during the six operating modes are depicted in Fig.7. The current regulation and detailed switching sequences are explained in Fig.8.The torque and speed control loop from which the required reference torque is obtained gives the reference current value. This is represented by the bold line. A smaller band causes higher switching frequency and lower toque ripple. Therefore, the upper and lower bands for hysteresis control are fixed based on these values.

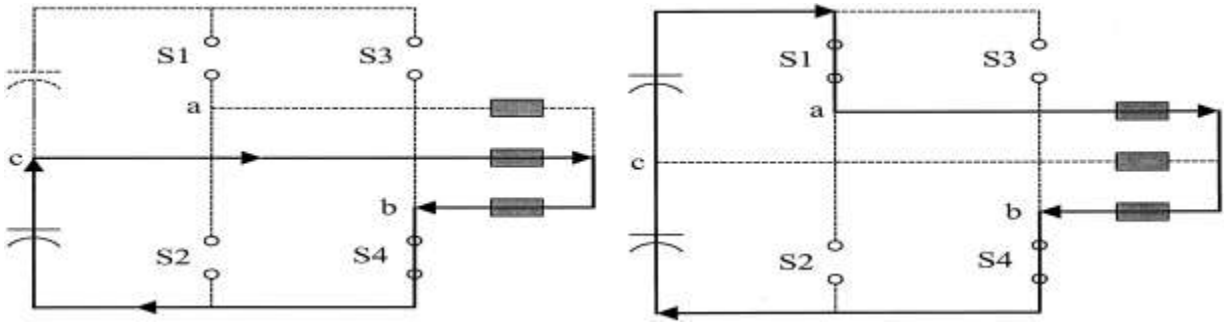

(a) (b)

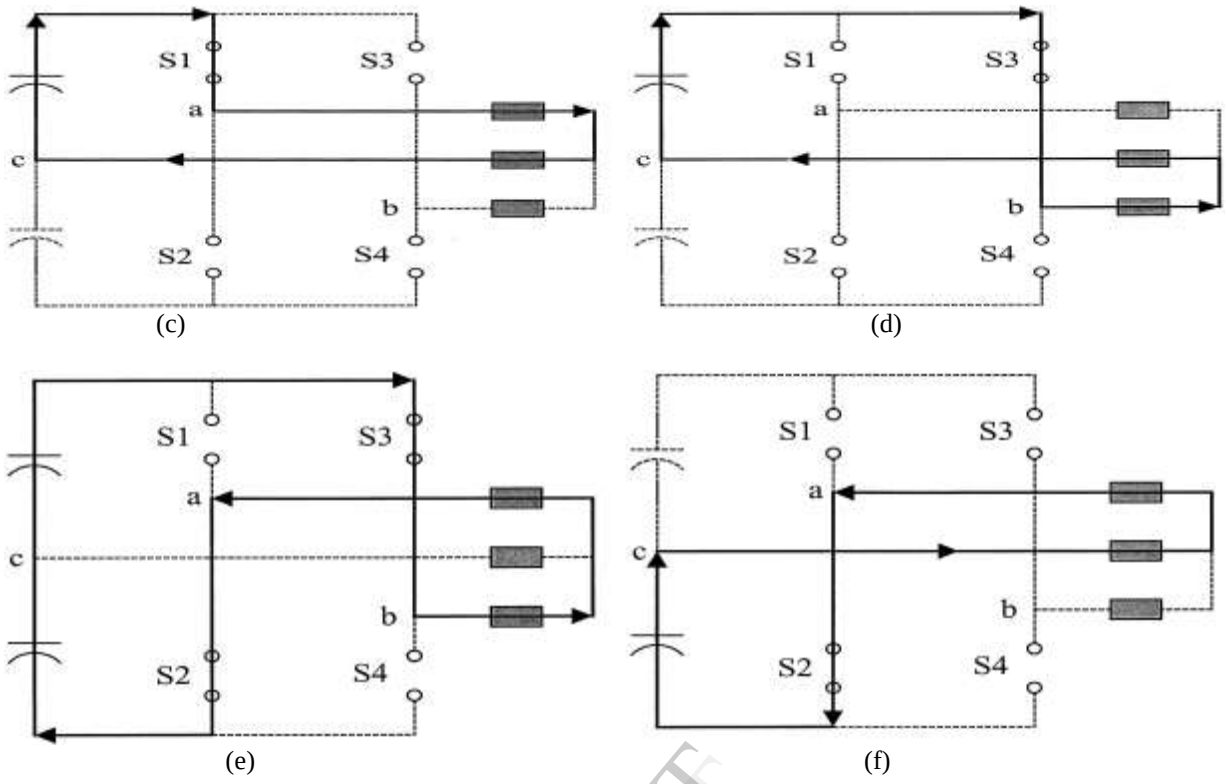

Fig.7. Direct current controlled PWM strategy for modes: (a)I:S_4,(b)II:S_1 & S_4,(c)III:S_1,(d)IV:S_3,(e)V:S_2 & S_3,(f)VI:S_2

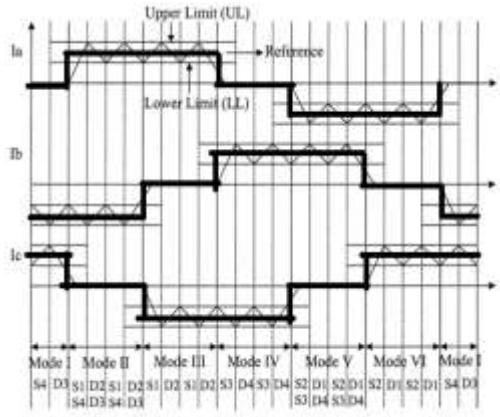

Fig.8. Switching sequence for current regulation

Considering phase A, we can take two cases as follows:

Case 1 : $I_a>0$

I^{st} Interval : $I_a<$ Lower Limit (LL); S_1 is ON

II^{nd} Interval : $I_a>$ Upper Limit (UL); S_1 is OFF

III^{rd} Interval : $LL<I_a<UL$ and $d/dt\ (I_a)>0$;S_1 is ON

IV^{th} Interval : $LL<I_a<UL$ and $d/dt\ (I_a)<0$;S_1 is OFF

Case 2 : $I_a<0$

I^{st} Interval : $I_a>UL$; S_2 is ON

II^{nd} Interval : $I_a<(LL)$; S_2 is OFF

III^{rd} Interval : $LL<I_a<UL$ and $d/dt\ (I_a)<0$;S_2 is ON

IV^{th} Interval : $LL<I_a<UL$ and $d/dt\ (I_a)>0$;S_2 is OFF

The same explanation can be given to phases B and C. Based on the current regulation, the voltage and current equations during the various modes are as shown in table III.

Table III

Voltage and current equations after current regulation

Modes	$di/dt>0$	$di/dt<0$
Mode I	$\frac{di_a}{dt}=-\frac{R}{L}i_a+\frac{1}{2L}(V_d-e_{ab})$	$\frac{di_a}{dt}=-\frac{R}{L}i_a-\frac{1}{2L}(V_d+e_{ab})$
Mode II	$\frac{di_a}{dt}=-\frac{R}{L}i_a+\frac{1}{2L}(2V_d-e_{ab})$	$\frac{di_a}{dt}=-\frac{R}{L}i_a-\frac{1}{2L}(2V_d+e_{ab})$
Mode III	$\frac{di_a}{dt}=-\frac{R}{L}i_a+\frac{1}{2L}(V_d-e_{ac})$	$\frac{di_a}{dt}=-\frac{R}{L}i_a-\frac{1}{2L}(V_d+e_{ac})$
Mode IV	$\frac{di_b}{dt}=-\frac{R}{L}i_b+\frac{1}{2L}(V_d-e_{bc})$	$\frac{di_b}{dt}=-\frac{R}{L}i_b-\frac{1}{2L}(V_d+e_{bc})$
Mode V	$\frac{di_b}{dt}=-\frac{R}{L}i_b+\frac{1}{2L}(2V_d-e_{bc})$	$\frac{di_b}{dt}=-\frac{R}{L}i_b-\frac{1}{2L}(2V_d+e_{bc})$
Mode VI	$\frac{di_c}{dt}=-\frac{R}{L}i_c+\frac{1}{2L}(V_d-e_{ca})$	$\frac{di_c}{dt}=-\frac{R}{L}i_c-\frac{1}{2L}(V_d+e_{ca})$

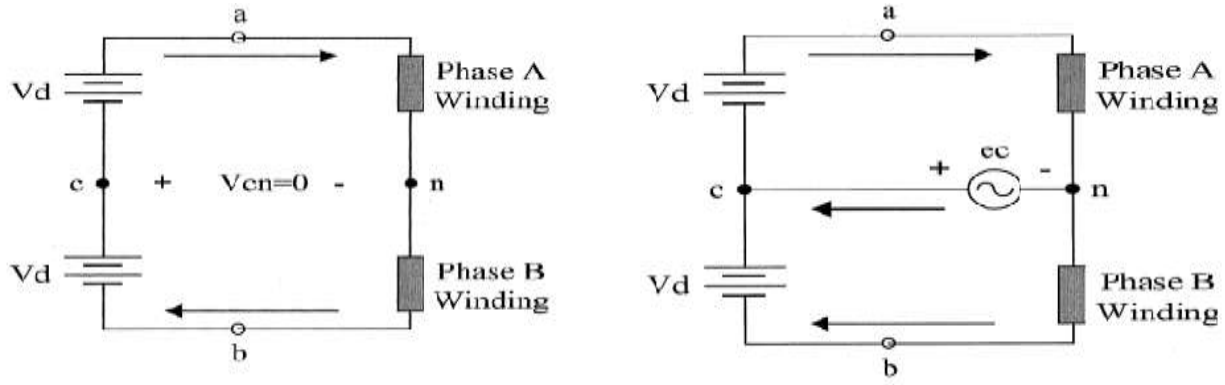

(a) (b)

Fig. 9.Simplified circuits showing modes II and V.(a)Ideal case. (b) Effect of back emf of phase C.

D. Back EMF compensation.

While examining modes II and V, it's seen that the active phases are phases A and B and the silent phase is phase C. That means, it's expected that the current through phase C is zero. But the back emf of phase causes an unexpected current to flow through phase C thereby distorting the actual currents in phases A and B. Therefore, while considering the direct current controlled PWM scheme, the back emf compensation problem should also be considered. Fig.9 illustrates the back emf compensation. In Fig.9 (a), the current through phases A and B are same. Therefore any one current need to be sensed, either the current through phase A or that through phase B. If the current through phase A is sensed, then, the switching signal of S_1 is determined independently and that of S_4 depends on the S_1 signal. So phase A current can be regarded as a constant current source. In this case, the current through phase B will be distorted due to the back emf of phase C.

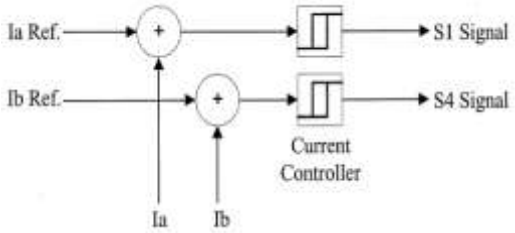

Fig.10.PWM strategy for Back EMF compensation.

Same is the case when phase B is controlled. Here, the current through phase A would be distorted by the back emf of phase C. From this it's deduced that the currents through phases A and B should be sensed and controlled independently as shown in Fig.10.This is called Direct Phase Current control scheme (DPC).

III. Sensorless control of fstpi bldc motor drive.

Terminal voltages of a BLDC motor in the four switch inverter with respect to the mid-point of DC bus as shown in Fig 3 are:

$$V_{ao}=Ri_a + Ld/dt\ (ia_) + e_a + V_{no}$$
$$V_{bo}=Ri_b + Ld/dt\ (ib_) + e_b + V_{no} \quad (5)$$
$$V_{co}=Ri_c + Ld/dt\ (ic) + e_c + V_{no}=0$$

The commutation instants are exactly 30° phase shifted from the zero crossing points of the back emf. However, creating a 30° phase shift results in more hardware or complicated software that can lead to computational errors. Therefore a novel position sensorless method is developed based on the line voltages of BLDC motor.

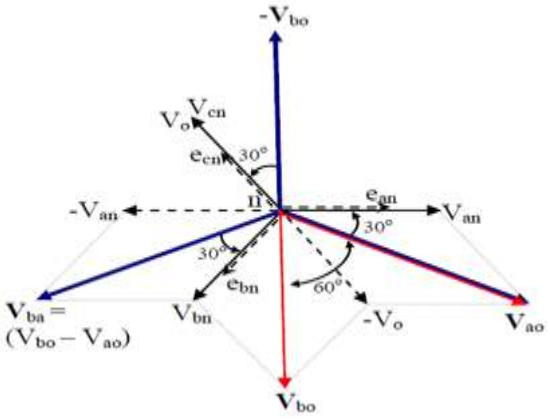

Fig.11.Phasor diagram of stator voltages of FSTPI BLDC motor drive

In a four-switch inverter topology, as shown in Fig.11, terminal voltages V_{ao} and V_{bo} are oriented 60° together. That means V_{ao} and $-V_{bo}$ lag 30° with respect to e_{an} and e_{cn} respectively. Moreover, voltage $V_{bo}-V_{ao}= V_{ba}$ also lag 30° with respect to e_{bn}. This means that the zero crossing points of V_{ao}, V_{ba} and $-V_{bo}$ can be used to commutate the currents in phase A, B and C respectively. Thus the three voltage functions (VF) derived from the two terminal voltages V_{ao} and V_{bo} are :

$$VF_a=V_{ao}$$
$$VF_b=V_{ba}=V_{bo}-V_{ao} \quad (6)$$
$$VF_c=-V_{bo}$$

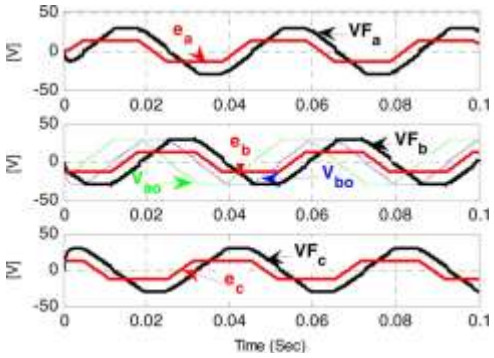

Fig.12. Voltage function and phase back emf voltages of FSTPI-BLDC motor drive.

Fig.12 shows the waveforms of voltage functions and phase Back emf voltages of BLDC motor drive. Zero crossings of VFs are detected using simple comparator circuits, and the virtual Hall sensor signals VH_a, VHb and VH_c are generated that can be used for current commutation. The virtual Hall sensor signals and the corresponding operation modes are summarized in table IV.

Table IV
Commutation logic from voltage functions

Voltage Function	VF_x sign before ZCP	VF_x sign after ZCP	Next mode	$H_cH_bH_a$
VF_b	Positive	Negative	I	100
VF_a	Negative	Positive	II	101
VF_c	Positive	Negative	III	001
VF_b	Negative	Positive	IV	011
VF_a	Positive	Negative	V	010
VF_c	Negative	Positive	VI	110

IV. Simulation results.

The implementation of four switch brushless dc motor drive system in simulink is shown in Fig.13.

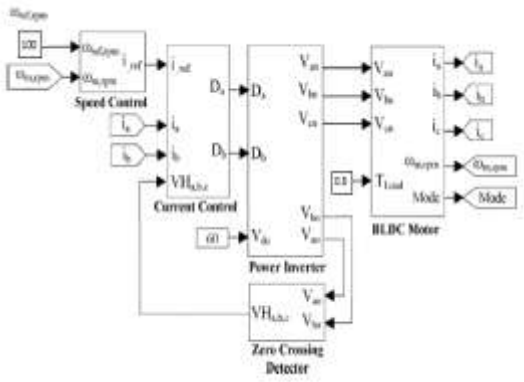

Fig.13.Simulink model of sensorless controlled FSTPI-BLDC motor

This is a high torque low speed motor with load torque as 0.5[Nm],reference speed as 100[rpm] and DC bus voltage as 60[v].The rated BLDC motor parameters are listed in table V.

Table V
Motor Specifications

P_n	425 [W]	Z_p	4 [pole]
T_n	10 [N.m]	ω_n	150 [rpm]
R	0.7 [Ω]	J	2e-4 [Kg. m^2]
L_s	2.72 [mH]	M	0.15 [mH]
K_t	1.194 [N.m/A]	K_e	0.5218 [V/rpm]

The main blocks used are Speed control block, Current control block, Power inverter block, BLDC motor block and Zero crossing detector block. The speed control block generates the reference current. The direct phase current control (DPC) scheme is employed in the current control block where the currents of two phases A and B are regulated through two independent current regulators. Proper phase voltages and terminal voltages are generated by the power inverter block and are applied to the BLDC motor block and Zero crossing detector block respectively using the developed duty cycle. Two second order low pass filters are used to eliminate the high frequency components. Virtual position Hall signals for sensorless control are then generated from the zero crossing points of voltage functions within the zero crossing detector block. Fig.14 shows the back emf waveforms of phase A, phase B and phase C. The rectangular phase currents are shown in Fig.15.Fig.16 shows the estimated operation modes and Virtual Hall Sensor signals VHa,VHb and VHc.

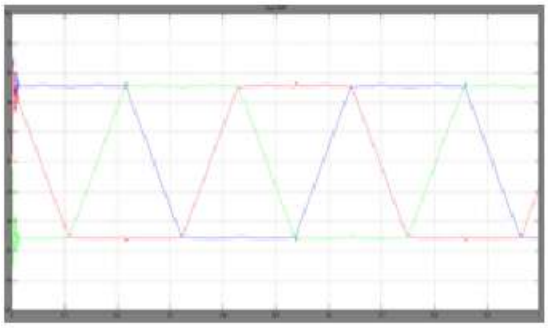

Fig.14.Back emf waveforms of the three phases.

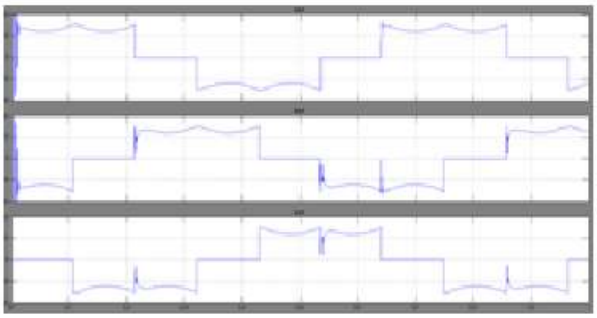

Fig.15. Rectangular phase current waveforms of phases A,B and C.

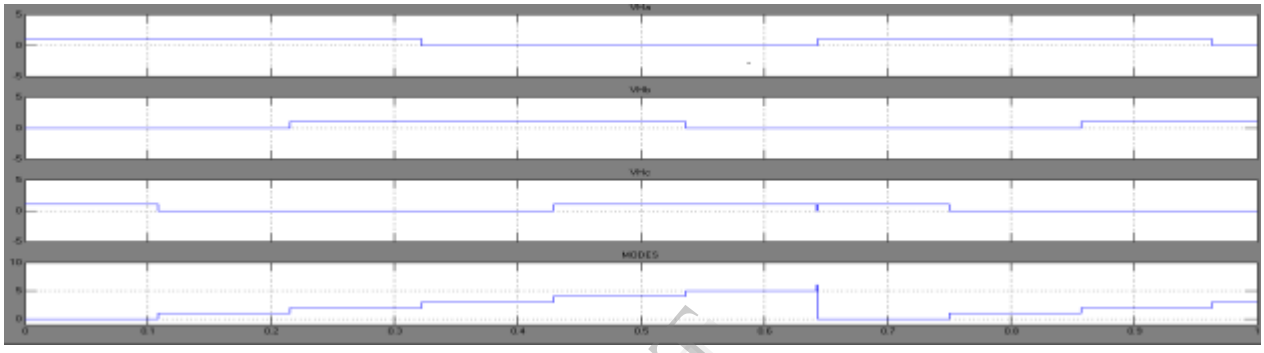

Fig.15.Virtual Hall sensor signals and operating modes.

V. Conclusion.

A four-switch converter topology is introduced in this paper where cost saving is achieved by reducing the number of inverter power switches and also by eliminating the position Hall-effect sensors and phase shifters.The measured terminal voltages yields the virtual Hall signals for current commutation thereby giving a sensorless control. Simulation validates the proposed sensorless method. The main advantages of the proposed method are:

- Simplification of power conversion circuit.
- Using four switch inverter, all the six commutation instants can be detected.
- This method can be applied to permanent magnet synchronous motors as it is independent of back emf waveforms.
- Phase shifters are not required as the virtual hall sensors immediately follows the commutation instants.

Therefore, the implementation of the proposed method is easier and less expensive than other sensorless methods.

References.

[1] P. Pillay and R. Krishnan, "Modeling, simulation, and analysis of permanent-magnet motor drives. II.The brushless DC motor drive," *IEEE Trans. Ind.Appl.*, vol. 25, no. 2, pp. 274–279, Mar./Apr. 1989.

[2] A.H Niasar, Abolfazl Vahedi, and Hassan Moghbelli, "A novel position sensorless control of a four switch Brushless DC motor drive without phase shifter," *IEEE Trans. Power Electron.*, vol. 23, no. 6, pp.3079–3087, Nov. 2008.

[3] B. K. Lee, T. H. Kim, and M. Ehsani, "On the feasibility of four-switch three-phase BLDC motor drives for low cost commercial applications:Topology and control," *IEEE Trans. Power Electron.*, vol. 18, no. 1, pp.164–172, Jan. 2003.

[4] J. P. Jahnson, M. Ehsani, and Y. Guzelaunler, "Review of sensorless methods for brushless DC," in *Proc. IEEE IAS Annu. Meeting Conf.*,1999, pp. 143–150.

[5] P. P. Acarnley and J. F. Watson, "Review of position-sensorless operation of brushless permanent-magnet machines,"*IEEE.Trans.Ind.Electron.*,vol.53,no.2,pp.352–362,Apr.2006.

[6] J. Shao, D. Nolan, and T. Hopkins, "A novel direct back EMF detection for sensorless brushlessDC(BLDC) motor drives," in *Proc.IEEE Appl.Power Electron. Conf. Expo.*, 2002, vol. 1, pp. 33–37.

[7]G. J. Su and W. McKeever,"Low-cost sensorless control of brushless DC motors with improved speed range," *IEEE*

Trans. Power Electron.,vol. 19, no. 2, pp. 296–302, Mar. 2004.

[8] G. Zhou, Z.Wu, and J. Ying, "Improved sensorless brushless DC motor drive," in *Proc. IEEE Power Electron. Spec. Conf. (PESC 2005)*, pp.1353–1357.

[9] C. Wang, G. Sung, K. Fang, and Sh. Tseng, "A low-power sensorless inverter controller of brushless DC motors," in *Proc. IEEE Int. Symp.Circuits Syst. (ISCAS,2007)*,pp.2435–2438.